THE JOURNAL OF BIOLOGICAL CHEMISTRY
Vol. 277, No. 49, Issue of December 6, pp. 47263–47269, 2002
Printed in U.S.A.

Intra- and Intermolecular Interactions between Intracellular Domains of Receptor Protein-tyrosine Phosphatases*

Received for publication, June 12, 2002, and in revised form, September 27, 2002
Published, JBC Papers in Press, October 9, 2002, DOI 10.1074/jbc.M205810200

Christophe Blanchetot, Leon G. Tertoolen, John Overvoorde, and Jeroen den Hertog‡

From the Hubrecht Laboratory, Netherlands Institute for Developmental Biology, Uppsalalaan 8, Utrecht 3584 CT, The Netherlands

The presence of two protein-tyrosine phosphatase (PTP) domains is a striking feature in most transmembrane receptor PTPs (RPTPs). The generally inactive membrane-distal PTP domains (RPTP-D2s) bind and are proposed to regulate the membrane-proximal PTP domains (RPTP-D1s). We set out to characterize the interactions between RPTP-D1s and RPTP-D2s *in vivo* by co-immunoprecipitation of hemagglutinin-tagged fusion proteins encoding the transmembrane domain and RPTP-D1 and myc-tagged RPTP-D2. Seven RPTPs from four different subfamilies were used: RPTPα, RPTPε, LAR, RPTPσ, RPTPδ, CD45, and RPTPμ. We found that RPTP-D2s bound to RPTPs with different affinities. The presence of intrinsic RPTP-D2 altered the binding specificity toward other RPTP-D2s positively or negatively, depending on the identity of the RPTPs. Furthermore, the C terminus of RPTP-D2s and the "wedge" in RPTP-D1s played a central role in binding specificity. Finally, full-length RPTPα and LAR heterodimerized in an oxidative stress-dependent manner. Like RPTPα-D2, the LAR-D2 conformation was affected by oxidative stress, suggesting a common regulatory mechanism for RPTP complex formation. Taken together, interactions between RPTP-D1s and RPTP-D2s are a common but specific mechanism that is likely to be regulated. The RPTP-D2s and the wedge structures are crucial determinants of binding specificity, thus regulating cross-talk between RPTPs.

Protein-tyrosine phosphorylation is of major importance for cell migration, proliferation, differentiation, and transformation within higher eukaryotic organisms. A common way to transmit extracellular signals into the cytoplasm is through receptor protein-tyrosine kinase (RPTK)[1] activation that consequently activates cytosolic proteins by protein-tyrosine phosphorylation. Tyrosine phosphorylation levels are negatively regulated by the protein-tyrosine phosphatases (PTPs) (1). The family of PTPs is divided into two large groups, the cytosolic PTPs and the transmembrane, receptor-like PTPs (RPTPs) (2, 3). Most of the RPTPs include two PTP domains, of which the membrane proximal domain (RPTP-D1) contains all or most of the PTP activity. An understanding of the conservation of the membrane distal PTP domain (RPTP-D2) has remained elusive for a long time. Recent reports suggest a regulatory instead of a catalytic function. Indeed, most of the RPTP-D2s are inactive or very weakly active (4). However, the structure of these RPTP-D2s is similar to that of RPTP-D1s (5), and mutation of only two residues, which are otherwise highly conserved in active PTPs, restored catalytic activity in several RPTP-D2s (5–8), suggesting that there is evolutionary pressure to keep RPTP-D2s inactive (8).

Biochemical and structural studies show that RPTP-D2s bind to RPTP-D1s in an intra- and intermolecular fashion. RPTPδ-D2 was found to directly inhibit RPTPσ-D1 activity through binding to the juxtamembrane region of RPTPσ-D1 (9). In addition, RPTPα binds to various RPTP-D2s, suggesting that cross-talk between RPTPs may be a shared mechanism of regulation (10). Inter- and intramolecular interactions between purified CD45-D1 and CD45-D2 suggest they are direct. CD45-D2 binding to CD45-D1 may disrupt CD45-D1/CD45-D1 homodimerization, perhaps leading to the CD45-D1 activation detected (11). Recently, the juxtamembrane region of RPTPμ was shown to bind in an intramolecular fashion with both PTP domains of RPTPμ, thus regulating RPTPμ-D1 activity (12, 13). Finally, the crystal structure of the complete cytoplasmic domain of LAR, containing LAR-D1 and LAR-D2, provided some structural evidence for intramolecular D1/D2 binding (5). LAR-D1 interacts extensively with LAR-D2 through the spacer region. Using intramolecular FRET, the conformation of RPTPα-D2 was found to change from a "closed" to an "open" conformation in an oxidative stress-dependent manner. The change in conformation has functional consequences, because only the open RPTPα-D2 binds intermolecularly with RPTP domains (14). However, whether RPTP-D1/RPTP-D2 binding is a general mechanism and, if so, with what specificity, is not known.

The function of RPTP-D1/RPTP-D2 binding may be to regulate RPTP-D1 activity, either directly or through regulation of RPTP-D1/RPTP-D1 dimerization. Several reports suggest that RPTP-D1 activity of RPTPα and CD45 is negatively regulated by dimerization (15–19). The crystal structure of RPTPα-D1 shows a direct reciprocal interaction of a helix-loop-helix "wedge" structure in the juxtamembrane region with the catalytic site of the opposing monomer (15). The juxtamembrane domain of RPTPσ and the wedge of RPTPα are involved in binding to RPTP-D2s (9, 10). Furthermore, CD45-D1 showed an increase in activity when fused to CD45-D2, presumably due to the increase in monomerization (11). The involvement of the wedge in RPTP-D1/RPTP-D2 binding suggested a possible role for RPTP-D2s in the regulation of RPTP-D1/RPTP-D1 dimer-

* This work was supported by the Research Council for Earth and Life Sciences with financial aid from the Netherlands Organization for Scientific Research. The costs of publication of this article were defrayed in part by the payment of page charges. This article must therefore be hereby marked "*advertisement*" in accordance with 18 U.S.C. Section 1734 solely to indicate this fact.

‡ To whom correspondence should be addressed. Tel.: 31-30-212-1800; Fax: 31-30-251-6464; E-mail: hertog@niob.knaw.nl.

[1] The abbreviations used are: (R)PTK, (receptor) protein-tyrosine kinase; (R)PTP, (receptor) protein-tyrosine phosphatase; D1, membrane-proximal PTP domain; D2, membrane-distal PTP domain; HA: hemagglutinin; FRET, fluorescence resonance energy transfer; aa, amino acid(s); PVDF, polyvinylidene difluoride; LAR, leukocyte common antigen related; CFP, cyan fluorescent protein; HARPTPα, hemagglutinin-tagged RPTPα; YFP, yellow fluorescent protein.

ization (10) or in direct regulation of the catalytic activity (9, 11).

Like RPTKs, RPTPs may form heterodimers *in vivo*. Studies on the Erb family of RPTKs showed that heterodimerization induced specific downstream events different than the ones induced by homodimerization (20, 21). To get basic insight into the relationship between RPTPs, we set out to identify binding between various RPTPs, including RPTPα, RPTPϵ, LAR, RPTPδ, RPTPσ, RPTPμ, and CD45, and their RPTP-D2s *in vivo*. We found that specific RPTP-D1/RPTP-D2 interactions were favored. The presence of intrinsic RPTP-D2 affected the binding specificity. Furthermore, we found that the C-terminal sequence, at least in RPTPδ-D2, and the wedge in RPTPα were critical to direct RPTPδ-D2 binding specificity suggesting multiple sites of interaction. Finally, we also show heterodimerization between full-length RPTPα and LAR in an oxidative stress-dependent manner. Taken together, we show that binding of RPTPs to RPTP-D2s are common but specific and that RPTP-D2s contain all the features necessary to drive the specificity of RPTP dimerization. Furthermore, our results suggest a specific mechanism of cross-talk between RPTPs.

EXPERIMENTAL PROCEDURES

Constructs—The transmembrane and first domain of different RPTPs were amplified by PCR using as template either mouse brain cDNA for RPTPσ, RPTPδ, and CD45 or cloned cDNA for HARPTPα (22), hLAR (gift of Wiljan Hendriks), hRPTPμ (gift of Wouter Moolenaar), and mRPTPϵ (gift of Ari Elson). PCR products were cloned into PSG5-13 to make HA-tagged fusion proteins as indicated in Fig. 1*A*. The following extracellular domains were cloned: the full extracellular domain of mRPTPα (amino acids (aa) 1–516, numbering according to Sap *et al.* (23)) and mRPTPϵ (aa 20–419, accession number P49446); the sequence from the cleavage site onward from hLAR (aa 1173–1610, accession number Y00815), mRPTPσ (aa 1176–1617, accession number D28530), and mRPTPδ (aa 568–1005, accession number D13903); hRPTPμ (aa 720–1179, accession number X58288) and mCD45 (aa 805–1152, accession number P06800) without an extracellular domain. PCR products encompassing different RPTP-D2s were cloned in pCS2+MT to make myc-tagged fusion protein, for the following RPTPs: mRPTPα (aa 537–793), mRPTPϵ (aa 456–717), hLAR (aa 1642–1897), mRPTPσ (aa 1648–1904), mRPTPδ (aa 1037–1292), hRPTPμ (aa 1200–1452), and mCD45 (aa 805–1152). For RPTPδ-D2fs a frameshift was introduced by a single base insertion at residue 1257 by site-directed mutagenesis and verified by sequencing.

Cell Cultures and Transfections—293 cells were routinely grown in DF medium (a 1:1 mixture of Dulbecco's modified Eagle's medium and Ham's F12 medium) supplemented with 7.5% fetal calf serum. Cells were transfected using the standard calcium-phosphate precipitation method. Briefly, 10-cm dishes were transfected with a total of 20 μg of DNA. The next day, the medium was refreshed and left for another 16 h before harvesting (22).

Immunoprecipitation and Immunoblotting—Sub-confluent transfected cells were washed twice with ice-cold phosphate-buffered saline, and lysed with cell lysis buffer, CLB (50 mM HEPES, pH 7.4, 150 mM NaCl, 1 mM $MgCl_2$, 10% glycerol, 1% Triton X-100, and protease inhibitors, including benzamidine, aprotinin, and leupeptin) for 20 min on ice, harvested, and centrifuged at 14,000 $\times$ *g* for 15 min to remove the insoluble fraction. The supernatant was added to 12CA5 antibodies coupled to Protein A-Sepharose. After 2 h of incubation at 4 °C, the beads were carefully washed 4$\times$ with HNTG buffer (20 mM HEPES, pH 7.4, 150 mM NaCl, 0.1% Triton X-100, 10% glycerol), mixed with 2$\times$ Laemmli buffer and loaded onto a 7.5% SDS-PAGE gel. The proteins were transferred to PVDF membrane using a semidry transfer system. After Coomassie Blue staining, the membrane was blocked for 1 h with 5% milk in TBS-Tween (50 mM Tris, pH 8.0, 150 mM NaCl, 0.05% Tween 20) at room temperature, incubated with the indicated first antibody (anti-HA, 12CA5; anti-myc 9E10 (Santa Cruz Biotechnology); anti-LAR (rabbit antibody raised against LAR-D2, gift of Wiljan Hendriks)), for 1.5 h, washed 4$\times$ with TBS-Tween, incubated with horseradish peroxidase-conjugated secondary antibody (anti-mouse or anti-rabbit, Transduction Laboratories) for 1 h, washed 4$\times$ with TBS-Tween, and developed using enhanced chemiluminescence (ECL).

FRET Analysis—CFP, YFP2.1 (24), and LAR-SpD2 (residues 1609–1897) were amplified by PCR and cloned in-frame using restriction sites. The resulting construct (CFP-LAR-SpD2-YFP) was checked by sequencing. 293 HEK cells were cultured on glass coverslips and transfected with CFP-LAR-SpD2-YFP. FRET was measured according to a previous study (14). In short, single cells were excited at 430 nm (a suboptimal excitation of CFP at 430 nm was chosen to minimize direct excitation of YFP), and the emission spectrum was recorded.

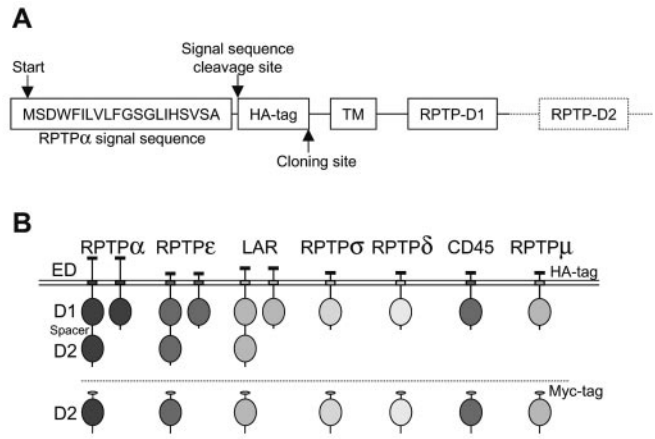

FIG. 1. **Constructs used in this study.** *A*, representation of the constructs used to clone the juxtamembrane and the first domain (and in some cases both PTP domains) of RPTPs (see "Experimental Procedures"). RPTPs were fused at the *cloning site*, downstream of the signal sequence of RPTPα, required for targeting to the plasma membrane, and an HA tag. During the translational process, the signal sequence is cleaved at the *signal sequence cleavage site*, exposing the HA tag. *B*, schematic representation of the constructs engineered. HA-tagged RPTP-D1s or HA-tagged RPTP-D1D2s are represented at the *top*. Myc-tagged RPTP-D2s are represented in the *lower part*.

RESULTS

RPTP-D1s and RPTP-D2s—We previously showed that RPTPα was able to bind to multiple RPTP-D2s, including RPTPα-D2, LAR-D2, RPTPσ-D2, and RPTPδ-D2 with various affinities (10). Multiple sites are involved in RPTP interactions (see the introduction). To investigate the possible role of RPTP-D2s in RPTP (hetero)dimerization, we asked how different isolated RPTP-D2s bound to different RPTP-D1s. For this purpose we used RPTPα, RPTPϵ, LAR, RPTPσ, RPTPδ, RPTPμ, and CD45. All RPTP-D2s were myc-tagged and were equivalent, in that they all started at residues equivalent to RPTPα residue 537 and did not contain the spacer region (region between D1 and D2) (Fig. 1*B*). The absence of the spacer region was crucial, because it released the RPTP-D2s from their inhibitory closed conformation and allowed interaction with RPTPs independently of stimulation (14). The differences in size between RPTP-D2s were due to small differences in size of the PTP domains as well as to small differences in the cloning procedures. The transmembrane domain and the first PTP domain (RPTP-D1) of RPTPα, RPTPϵ, LAR, RPTPσ, RPTPδ, RPTPμ, and CD45 were cloned in-frame with the signal sequence of RPTPα and a HA tag. The signal sequence ensured membrane targeting but did not interfere with the protein, because it is cleaved off during processing of the fusion protein at the membrane, exposing the HA tag (Fig. 1*A*). Small extracellular domains were included (for RPTPα and RPTPϵ), whereas large extracellular domains from the other RPTPs were not included to avoid possible disturbance. For LAR, RPTPσ, and RPTPδ whose ectodomain is cleaved, the sequence from the cleavage site onward was used (25). Similarly, constructs encoding the transmembrane and full intracellular domain (RPTP-D1D2) of RPTPα, RPTPϵ, and LAR were cloned (Fig. 1*B*).

Interaction between RPTP-D1s and RPTP-D2s—Routinely, 293 cells were transiently co-transfected with HA-tagged

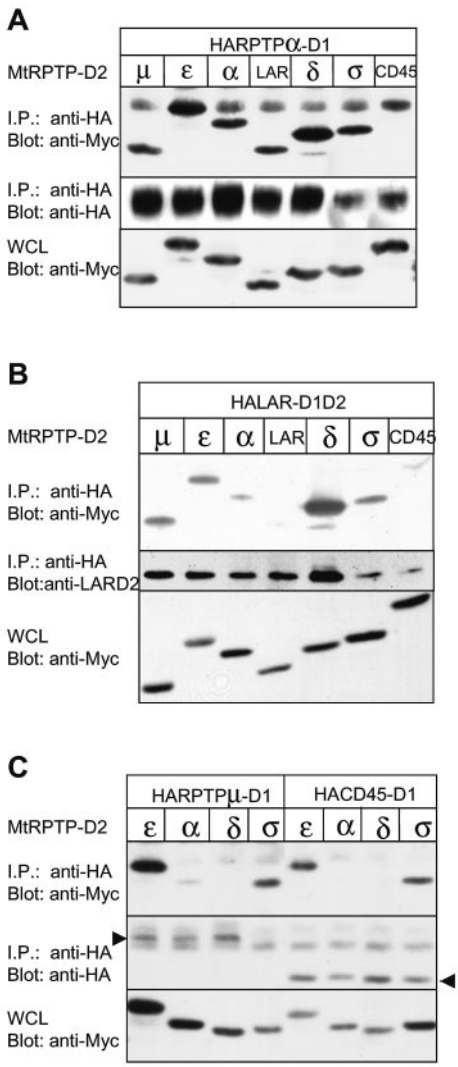

FIG. 2. **Specific binding between RPTP-D1s and RPTP-D2s.** *A*, 293 cells were co-transfected with RPTPα lacking its second domain (HARPTPα-D1) and the myc-tagged second domains of the indicated RPTPs (MtRPTP-D2). After anti-HA immunoprecipitation, separation on SDS-PAGE, and transfer onto a PVDF membrane, the blot was probed with anti-Myc antibodies to test for co-immunoprecipitated MtRPTP-D2s (*top panel*) and with anti-HA antibodies for HARPTPα-D1 (*middle panel*). Expression of the myc-tagged RPTP-D2s was monitored in the *lower panel*. *B*, HALAR-D1D2 was co-transfected with different RPTP-D2s (similar as in *A*). After anti-HA immunoprecipitation, the blot was probed as indicated. *C*, a subset of myc-tagged RPTP-D2s (MtRPTP-D2) was co-transfected in 293 cells with HARPTPμ-D1 or HACD45-D1 as indicated. After anti-HA immunoprecipitation, the blot was probed with anti-Myc antibodies to test for co-immunoprecipitated MtRPTP-D2s (*top panel*) and for HARPTP-D1s using anti-HA antibodies (*middle panel*); *arrowheads*. Expression of the Myc-tagged RPTP-D2s was monitored in the *lower panel*. *I.P.*, immunoprecipitation; *WCL*, whole cell lysate.

RPTP-D1 constructs together with the panel of myc-tagged RPTP-D2s to detect differences in affinities. The HA tag was used for immunoprecipitation, and co-immunoprecipitated myc-tagged RPTP-D2s were detected. Typical results of a co-immunoprecipitation assay are depicted in Fig. 2. Note that an intrinsic difficulty of such an *in vivo* approach is to reach equivalent protein expression. Therefore, the expression levels were monitored to allow for corrections. RPTPα-D1 bound all RPTP-D2s tested, although with different affinities (Fig. 2*A*). RPTPϵ-D2 and RPTPδ-D2 bound with higher affinity to RPTPα-D1, relative to other RPTP-D2s. The differences in binding affinity were more extreme for LAR-D1D2 (Fig. 2*B*). RPTPδ-D2 bound strongly to LAR-D1D2, as did RPTPϵ-D2, whereas CD45-D2 and LAR-D2 bound only weakly. Furthermore, RPTPμ-D1 and CD45-D1 bound efficiently to RPTPϵ-D2 and RPTPσ-D2, although RPTPμ-D1 was not always equally expressed (Fig. 2*C*). Binding to other RPTP-D2s was observed as well (*e.g.* RPTPα-D2, Fig. 2*C*), but the relatively low expression of the HA-tagged constructs made it difficult to detect. It is noteworthy that RPTPσ-D1 bound to RPTPσ-D2 (and RPTPϵ-D2, Table I) but not to RPTPδ-D2, contrary to results from Wallace *et al.* (9). Several reasons may explain these apparent differences: we used (i) membrane-localized RPTP-D1s that (ii) did not contain the spacer region (region between RPTP-D1 and RPTP-D2). Because the spacer region is involved in the stabilization and regulation of the intramolecular structure, this region may be of particular importance in the differences observed. In conclusion, we developed a system that can be used routinely for the detection of the *in vivo* interaction of RPTP-D1s with RPTP-D2s and show that RPTP-D1 binding to RPTP-D2s may be a common (but specific) mechanism within the RPTP family.

Effect of Endogenous D2 on Binding to Other RPTP-D2s—We further investigated the binding of RPTP-D2s to the full intracellular domain of RPTPα, RPTPϵ, and LAR. For most RPTP-D2s the binding pattern to the full intracellular domain (RPTP-D1D2) was similar to that of binding to RPTP-D1. Significant differences were found for LAR and RPTPϵ binding to RPTPδ-D2 and RPTPσ-D2. Although full-length RPTPϵ (RPTPϵ-D1D2) bound RPTPσ-D2 relatively well and RPTPδ-D2 more weakly, RPTPϵ-D1 bound more efficiently to RPTPδ-D2 than RPTPσ-D2 (Fig. 3*A* and Table I). The opposite effect was found with LAR. LAR-D1D2 bound preferentially to RPTPδ-D2, whereas LAR-D1 bound preferentially to RPTPσ-D2 (Fig. 3*B* and Table I). As a control, RPTPϵ-D2 always bound strongly to LAR-D1D2 and LAR-D1 (Fig. 3*B*). The same was true for RPTPϵ binding to RPTPϵ-D2 (Table I). This suggests that the presence of intrinsic D2 alters binding to some but not all RPTP-D2s. Whether the effect is positive or negative depends on the identity of the RPTPs.

A Matrix of Interactions between RPTP-D1s and RPTP-D2s—We repeated the co-immunoprecipitation experiments several times for each RPTP, leading to a good understanding of the interactions between RPTP-D1s (or RPTP-D1D2) and RPTP-D2s. The results presented in Table I were derived from the comparison of binding of RPTP-D2s to one HA-tagged RPTP at a time. However, because of the high number of variables, these data should be used qualitatively rather than quantitatively. We did not attempt to compare binding of one RPTP-D2 to all HA-tagged constructs because of the variation in HA-tagged protein expression and their pattern after immunoblotting (some proteins are single sharp bands, whereas some are more or less diffuse). Furthermore, each experiment was done separately, making comparison between blots impossible. Therefore, the data in the rows in Table I may be compared directly, whereas the data inside a column cannot be compared directly. However, patterns in rows may be compared with each other.

All RPTP-D2s tested interacted with multiple RPTP-D1s. RPTPϵ-D2 and RPTPσ-D2 always bound relatively well to all RPTP-D1s tested. RPTPδ-D2 bound either strongly (to RPTPα, RPTPϵ, or LAR-D1D2) or not at all (to the other RPTPs). RPTPα-D2 and RPTPμ-D2 bound with relatively similar but weak affinity to all RPTP-D1s tested. LAR-D2 and CD45-D2 also have a similar binding pattern and bound weakly to some but not to other RPTPs. In conclusion, our results suggest that RPTP-D2s have different patterns of binding to RPTP-D1s with different affinities. Taken together, our results support the

TABLE I
A matrix of interactions between RPTP-D1s and RPTP-D2s

293 cells were transiently cotransfected with HA-tagged RPTP (HA tag) constructs together with a panel of Myc-tagged RPTP-D2s as indicated (see Fig. 1). After anti-HA co-immunoprecipitation, the co-immunoprecipitated Myc-tagged RPTP-D2s were detected by immunoblotting. The interactions in the *same row* were scored relative to each other from not detectable (−), weak (+/−), and strong to very strong (gradually from + to ++++). The table depicted is the result of multiple independent experiments (*n*) as indicated. Because expression of the different constructs was variable, only results within experiments should be compared. Therefore, the data in the *rows* in this table may be compared directly, whereas the data in the *columns* should not be compared directly. However, patterns in *rows* may be compared to each other.

HA tag		Myc-tagged RPTP-D2s						
		RPTPα	RPTPε	LAR	RPTPδ	RPTPσ	RPTPμ	CD45[b]
RPTPα	D1	+	+++	++	+++	++	+	+
n = 4	D1D2	+	+++	+	++++	++	+	+
RPTPε	D1	++	+++	+	+++[a]	++[a]	+	+
n = 4	D1D2	+	+++	+	+[a]	++[a]	+	+
LAR	D1	+	+++	+	−[a]	+++[a]	++	+
n = 3	D1D2	+	++	−	+++[a]	++[a]	++	+/−
RPTPδ *n* = 1	D1	−	+++	+/−	−	+++	+	NT[c]
RPTPσ *n* = 3	D1	+/−	+++	−	−	+++	++	−
RPTPμ *n* = 3	D1	+	+++	−	−	+++	+	+/−
CD45 *n* = 2	D1	+/−	+++	−	−	+++	+/−	−

[a] Note the differences in binding patterns of RPTP-D1s and RPTP-D1D2s to the highly homologous RPTPδ-D2 and RPTPσ-D2.
[b] MtCD45-D2 migrates very close to an occasional background band disturbing MtCD45-D2 detection. Binding is thus presumably underestimated.
[c] NT, Not tested.

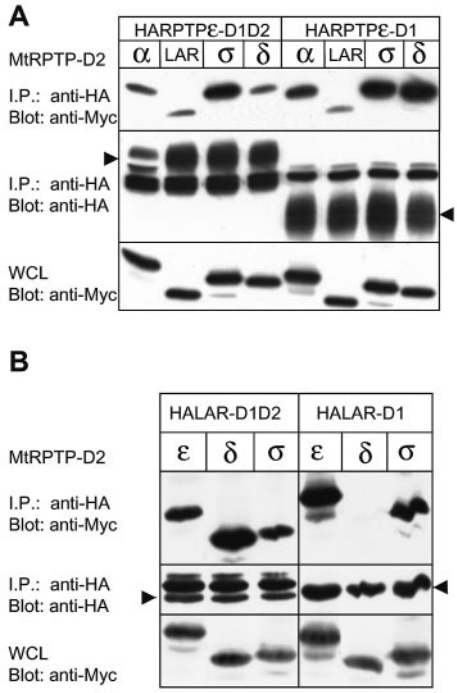

FIG. 3. **Effect of intrinsic RPTP-D2 on binding to other RPTP-D2s.** *A*, 293 cells were co-transfected with HARPTPε full intracellular domain (HARPTPε-D1D2) or HARPTPε lacking its second domain (HARPTPε-D1) and Myc-tagged RPTP-D2s (MtRPTP-D2) as indicated. After anti-HA immunoprecipitation, the blot was probed with anti-Myc antibodies to test for co-immunoprecipitated MtRPTP-D2s (*top panel*) and for HARPTPs using anti-HA antibodies (*middle panel*); *arrowheads*. Expression of the Myc-tagged RPTP-D2s was monitored in the *lower panel*. *B*, 293 cells were co-transfected with HALAR (HALAR-D1D2) or HALAR lacking its second domain (HALAR-D1) and Myc-tagged RPTP-D2s (MtRPTP-D2) as indicated. Immunoprecipitation and immunoblotting were as in *A*. HALARD1D2 or HALAR-D1 are indicated by *arrowheads*.

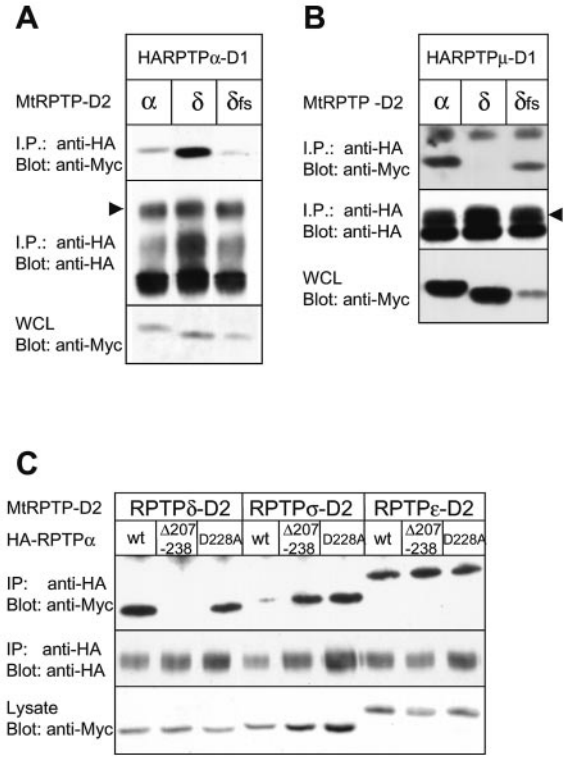

FIG. 4. **Determinants of binding specificity.** *A*, 293 cells were transiently co-transfected with HARPTPα-D1 (or HARPTPμ-D1 in *B*, *arrowheads*) and myc-tagged RPTP-D2 of RPTPα (α), RPTPδ (δ), or mutant RPTPδ with a frameshift leading to replacement of the C-terminal sequence (*δfs*). The HA-tagged proteins were immunoprecipitated using anti-HA antibody, and the blots were probed with anti-myc antibody (*top panel*) and anti-HA antibody (*middle panel*). Expression of the Myc-tagged-RPTP-D2s in the lysate was monitored (*bottom panel*). *C*, HARPTPα (*WT*), HARPTPαΔ207–238 (*Δ207–238*), or HARPTPα D228A (*D228A*) were co-transfected with myc-tagged RPTP-D2s as indicated. Co-immunoprecipitation and immunoblotting was done as in *A*.

idea that RPTP-D1s and RPTP-D2s of different RPTPs interact with each other suggesting specific cross-talk between RPTPs.

Specificity Determinants—We investigated which residues in RPTP-D2s were likely to be involved in the difference in affinity observed. RPTPδ-D2 bound better to RPTPα than RPTPα-D2 but also than RPTPσ-D2 and LAR-D2 despite their very high sequence homology (Fig. 2 and Ref. 10). Sequence comparison of RPTP-D2s revealed one particular residue that was conserved between mRPTPδ and rRPTPδ (9) and that at the same time was highly divergent between other RPTPs: LAR, RPTPσ, and RPTPα (data not shown). Thus, this residue, RPTPδ-Met-1257, was a good candidate to explain the differences in affinity observed. Unfortunately, point mutation of

TABLE II
Involvement of the C terminus in binding of RPTPδ-D2 to RPTPs
The interactions were scored as in Table I, from not detectable (−), weak (+/−), and strong to very strong (gradually from + to ++++).

HA tag		Myc-tagged RPTP-D2s		
		RPTPα	RPTPδ	RPTPδfs
RPTPα	D1	+	+++	+
	D1D2	+	++++	+
LAR	D1	+	−	+
	D1D2	+	+++	+
RPTPμ	D1	++	−	++

RPTPδ-Met-1257 to Ser, the corresponding residue in RPTPα, had no effect (data not shown). Introduction of a frameshift in RPTPδ at Met-1257 by insertion of a single base led to replacement of the C-terminal 35 residues of RPTPδ (α6 in the LAR crystal structure (5)) by non-related sequence of similar length (RPTPδ-D2fs). After co-immunoprecipitation with HARPTPα, only RPTPδ-D2 bound very strongly to HARPTPα, whereas binding of the frameshift mutant RPTPδ-D2fs was significantly reduced to levels in the same order of magnitude as RPTPα-D2 (Fig. 4*A*). The frameshift mutation not only reduced but also enhanced binding to some RPTP-D1s. Although no interaction between RPTPμ-D1 and RPTPδ-D2 was detected, RPTPμ-D1 bound efficiently to RPTPδ-D2fs (Fig. 4*B*). Similarly, RPTPδ-D2 did not bind to LAR-D1, whereas RPTPδ-D2fs did (Table II). In conclusion, these results show that the C terminus of RPTPδ-D2 affects binding of RPTPδ-D2 to RPTPs positively and negatively, and we conclude that the C terminus of RPTP-D2s is an important determinant of the specificity for RPTP-D1 and RPTP-D2 binding.

To get better insight into the function of RPTP-D2s binding to RPTP-D1, it is important to define the binding site within RPTP-D1. We previously showed that although the wedge structure of RPTPα-D1 is a binding site for RPTP-D2s in yeast two-hybrid and in glutathione *S*-transferase pull-down experiments (10), multiple sites of interactions exist *in vivo*. Indeed, deletion of the wedge of RPTPα (Δ204–235) does not prevent binding to most RPTP-D2s tested and even seems to favor RPTP-εD2 and RPTP-σD2 binding (Fig. 4*C* and Ref. 10). In contrast, the same deletion abolished binding of RPTPδ-D2 to RPTPα. It is noteworthy that a point mutation in the wedge of RPTPα (D228A) was not sufficient to affect RPTPδ-D2 binding. These results suggest that multiple binding sites exist between RPTP-D1 and RPTP-D2s and that some RPTP-D2 have different preferences for specific types of interactions.

Inducible Heterodimerization of Full-length RPTPs—Because there are multiple sites of interaction between RPTPs, it is necessary to study the RPTP domains separately to understand their binding specificity. However, it remained to be established whether heterodimerization occurs *in vivo* between (full-length) RPTPs. Although RPTPα dimers have been detected in living cells (26), we found that oxidative stress stimulation greatly increased co-immunoprecipitation of full-length RPTPα (14). Oxidative stress induced a conformational change in RPTPα leading to stabilization of RPTPα dimers and to complete inactivation of RPTPα. Reactive oxygen species are produced in response to many stimuli, and reactive oxygen species-mediated enhanced dimerization and inactivation of RPTPs may be an important regulatory mechanism for RPTPs. Therefore, we asked if heterodimerization between RPTPs might also be dependent on extracellular stimuli. LAR and HA-tagged RPTPα were transiently co-transfected in 293 cells, and binding was assessed by co-immunoprecipitation. Although no co-immunoprecipitation was detected in unstimulated cells, oxidative stress led to a large increase in RPTPα/LAR heterodimers (Fig. 5). Binding was specific, because an

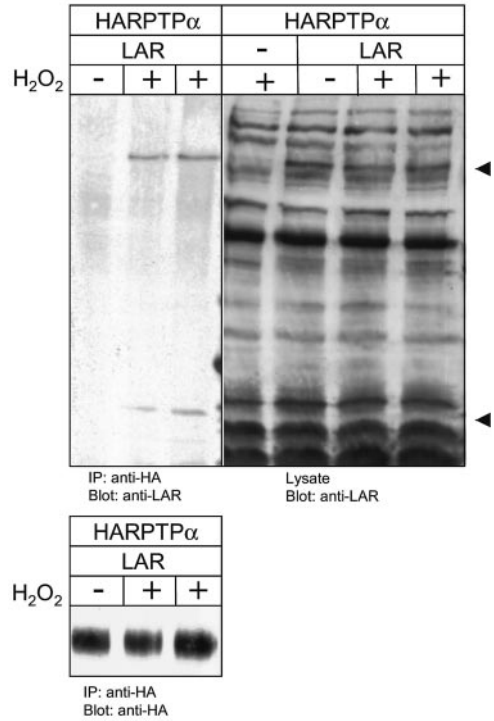

FIG. 5. **Inducible heterodimerization of RPTPα and LAR.** *A*, 293 cells were transiently co-transfected with HARPTPα and LAR, treated (+) or not (−) with 1 mM H_2O_2 for 5 min. After anti-HA immunoprecipitation, separation on SDS-PAGE, and transfer onto a PVDF membrane, co-immunoprecipitated LAR (*left*) and LAR present in the lysate (*right*) were detected on blot with anti-LAR-D2 antibody. Full-length LAR (~200 kDa) and the cleaved form of LAR (~80 kDa) are indicated with *arrowheads*. The amount of HARPTPα immunoprecipitated was monitored with anti-HA antibody (*bottom panel*).

increase in the amount of immunoprecipitated HARPTPα also increased the amount of co-immunoprecipitated LAR (Fig. 5, compare *lanes 2* and *3*). Furthermore, mutation of the second catalytic site cysteine (the residue required for the oxidative stress-induced conformational change) in RPTPα largely reduced the formation of a stable interaction between RPTPα and LAR (data not shown). These results show that full-length RPTPs can be induced to form heterodimers.

The requirement of oxidative stress may be explained by the "opening" of RPTPα allowing intermolecular interactions with LAR. Whether similar changes in the conformation of LAR also occur is not known. We used fluorescence resonance energy transfer (FRET) to study the effect of oxidative stress on the conformation of LAR-SpD2 ("Sp" represents the presence of the spacer region, the region between RPTP-D1 and RPTP-D2, see Fig. 1). Reminiscent of what was found with RPTPα-SpD2 (14), FRET was observed when a chimeric protein was engineered, CFP-LAR-SpD2-YFP, where CFP and YFP were fused (N- and C-terminally, respectively) to LAR-SpD2 (Fig. 6). This indicates that CFP and YFP are located very close to each other (<40–50 Å) in the protein, consistent with the LAR crystal structure (5). The weaker FRET prior to stimulation observed within CFP-LAR-SpD2-YFP (ratio 520/480 nm is around 1.4, see Fig. 6, *inset*) compared with CFP-RPTPα-SpD2-YFP (ratio 520/480 nm is ~2.5, see Ref. 14) might reflect a less optimal orientation of CFP toward YFP or less flexibility in the structure of RPTPα-SpD2. Oxidative stress reduced FRET (as detected by a reduction of the YFP emission and a concomitant increase in CFP emission due to the reduction in energy transfer from CFP to YFP) within CFP-LAR-SpD2-YFP (ratio 520/480 nm after H_2O_2 was ~1.2, which is similar to the value observed with CFP-RPTPα-SpD2-YFP after peroxide (14)), in-

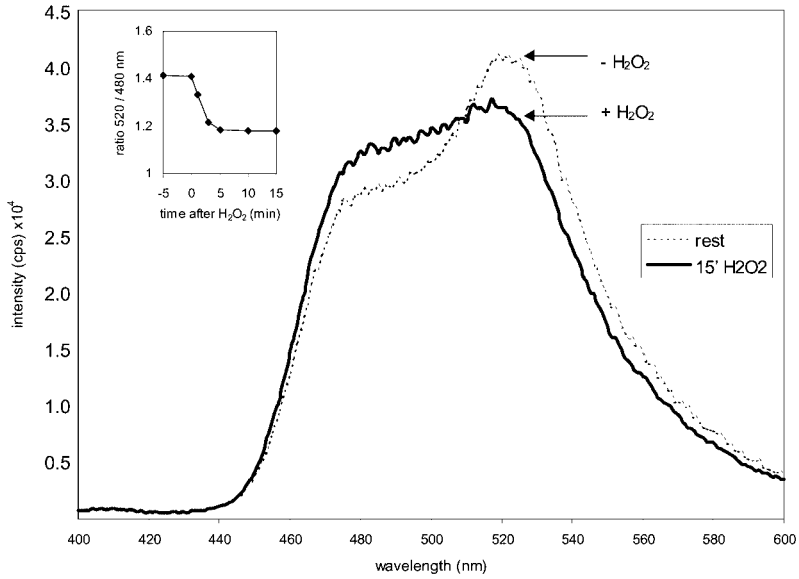

FIG. 6. **H_2O_2-induced conformational change in LAR-D2.** Emission spectra of a single transfected 293 human embryonic kidney cell (excitation 430 nm), expressing wild type CFP-LAR-SpD2-YFP before (*rest*) and after incubation with 1 mM H_2O_2 for 15 min. Note that the intensity of YFP decreases and the intensity of CFP increases after treatment. *Inset*, time course of FRET in response to stimulation with H_2O_2 for 0–15 min, indicated as the ratio of the emission intensities at 525 and 480 nm.

dicating that a conformational change also occurred within LAR-SpD2 (Fig. 6). Taken together, these results suggest that a conformational change in both RPTPα and LAR is involved in oxidative stress-induced heterodimerization of full-length RPTPα and LAR.

DISCUSSION

Like RPTKs, RPTPs may be regulated by dimerization (27). Even though multiple regions may be involved in RPTP dimerization, an important component for dimerization is RPTP-D2. RPTPδ-D2 binds to RPTPσ-D1 (9), different RPTP-D2s bind to RPTPα (10), and CD45-D2 and RPTPμ-D2 bind to their respective RPTP-D1s. Furthermore, the fact, that the so-called wedge structure, which interacts with the catalytic site of RPTP-D1 in the RPTPα dimer (15), also binds to RPTP-D2s (9, 10), suggests that RPTP-D2s may be involved in the regulation of dimerization (in *trans*) (10). Our results form the basis of a matrix of *in vivo* binding between RPTPs and RPTP-D2s. Such a matrix shows that all RPTP-D2s tested bound to membrane-localized RPTP-D1s but with different affinities. Apparently, four different patterns exist for RPTP/RPTP-D2 binding (Table I): 1) RPTPϵ-D2 and RPTPσ-D2 always bound relatively well to all RPTP-D1s tested; 2) RPTPδ-D2 bound either strongly (to RPTPα, RPTPϵ, or LAR-D1D2) or not at all (to the other RPTPs); 3) RPTPα-D2 and RPTPμ-D2 bound with relatively similar but weak affinity to all RPTP-D1s tested; and 4) LAR-D2 and CD45-D2 also have a similar binding pattern and bound weakly to some but not to other RPTPs. Very closely related RPTP-D2s have significantly different binding properties. RPTPϵ-D2 bound strongly to all RPTP-D1s, whereas RPTPα-D2, the closest homologue of RPTPϵ-D2, bound with much less affinity. Furthermore, LAR-D2, RPTPσ-D2, and RPTPδ-D2 have very different binding affinities, while they all share very high sequence homology. LAR-D2 bound weakly but specifically to RPTPs. RPTPσ-D2 bound strongly to all RPTPs tested, whereas RPTPδ-D2 bound strongly to some RPTPs, but not at all to others. Taken together, our results show that RPTP-D2s have all the characteristics for being at the base of the specificity of RPTP dimerization. Furthermore, our results show that accurate predictions of RPTP-D1/RPTP-D2 interactions based on sequence comparison is still not possible, putting emphasis on our experimental approach to unravel RPTP-D1/RPTP-D2 interactions and function.

The presence or absence of intrinsic RPTP-D2 affected the binding efficiency between the remaining RPTP-D1 and other RPTP-D2s. For instance, LAR-D1D2 preferentially bound RPTPδ-D2 while LAR-D1 preferentially bound RPTPσ-D2 (Fig. 3*B*). These results are consistent with the model that intramolecular D1/D2 binding regulates intermolecular D1/D2 interactions. Indeed, it was shown for CD45 and RPTPμ that the juxtamembrane region and the spacer region, when fused to RPTP-D1, alter the binding specificity of D1 toward RPTP-D2 (12, 30). Furthermore, we previously showed that the spacer region and the C-terminal region of RPTPα-D2 bind intramolecularly and regulate the interaction between RPTPα-D1 and RPTPα-D2 (14). Because the binding specificity of RPTP-D1s is different than RPTP-D1D2s, our results suggest that stimuli may induce a reshuffling of RPTP dimers.

We have previously shown that the C terminus of RPTPα-D2 was involved in binding to RPTPα (10). Using RPTPδ-D2, we further show the importance of the C terminus in RPTP-D2s and of the wedge in RPTP-D1s. Replacement of the C-terminal sequence of RPTPδ-D2 changed the binding specificity and affinity. The corresponding region in LAR forms a helix that is localized at the interface between LAR-D1 and LAR-D2 in the crystal structure (5), providing structural support that this region is somehow involved in intramolecular RPTPD1/RPTPD2 binding. The fact that mutation of this region positively and negatively altered the binding efficiency of different RPTPs may suggest that the C terminus forms (part of) the binding site for RPTP-D1s or plays an indirect role (by regulating RPTP-D2 opening). Other sites are involved in RPTP-D1/RPTP-D2 binding as well, because replacement of the C terminus increased binding in some cases. These results suggest that multiple binding sites between RPTP-D1 and RPTP-D2s exist and may compete and/or cooperate. The juxtamembrane region (Fig. 4*C* and Refs. 9 and 10), the C-terminal region (Fig. 4 and Ref. 10), and the spacer region (5, 12, 14, 30) are all involved in RPTP-D1/RPTP-D2 binding. The differences in binding between constructs may be due to differences in binding efficiency to one or more binding sites. A matrix such as the one described here may help to pinpoint specific binding sites or help to define these sites.

Homodimerization of RPTPα and CD45 is now well established. However, we found that oxidative stress stimulation was necessary to allow co-immunoprecipitation of full-length RPTPα dimers (14). Oxidative stress induced a change in the conformation of RPTPα-D2 that released RPTPα from a closed to an open conformation allowing stabilization of dimers. Here

we show that oxidative stress induced formation of heterodimers between full-length RPTPα and LAR as well. Using FRET, we demonstrated that oxidative stress induced a conformational change in LAR-D2 as well, albeit to a lesser extent than in RPTPα-D2. Although this was the first time that full-length RPTP heterodimers were detected, cross-talk between RPTPs has been proposed before. Importantly, several elaborate studies on *Drosophila* axon pathfinding clearly indicate functional cooperation and competition between RPTPs (28, 29). Although these studies only show genetic interactions, it is now tempting to speculate that cross-talk between *Drosophila* RPTPs may be mediated by direct, stimulation-dependent heterodimerization.

A burning question that remains is: what is the effect of RPTP-D2 on RPTP-D1 activity? RPTPδ-D2 binding inhibits RPTPσ-D1 (9), and RPTPμ-D2 binding decreases RPTPμ-D1 catalytic activity (12, 13). In contrast, the presence of CD45-D2 fused to CD45-D1 led to an increase in total PTP catalytic activity, presumably due to an increase in monomerization (11). Furthermore, *in vitro* no changes in RPTPα-D1 activity were detected after addition of RPTPα-D2 (data not shown). Taken together, these results suggest that the effect of RPTP-D2s on RPTP-D1s may depend on the RPTP, or on the RPTP-D1/RPTP-D2 combination. Indeed, the strength and site(s) of the interaction may be important. Strong binding of RPTP-D2 to the wedge may lead to inactivation of RPTP-D1, whereas weak and dynamic RPTP-D2 binding to the wedge may lead to monomerization and activation of RPTP-D1. For these reasons, all RPTP-D1/RPTP-D2 combinations will need to be studied for changes in activity. However, these activity assays are technically difficult, because the stoichiometry of binding of RPTP-D1 to RPTP-D2 will influence the effect of RPTP-D2 on RPTP-D1 activity in assays *in vitro*. A much-preferred configuration would require analysis of dephosphorylation of physiological substrates in living cells, which is not feasible yet for all RPTPs.

In conclusion, our results suggest that specific and regulated heterodimerization between RPTPs occurs *in vivo*. RPTP-D2s have specific affinity for RPTP-D1s and consequently may be at the base of functional and regulatory cross-talk between RPTPs.

Acknowledgments—We thank Wiljan Hendriks for providing the hLAR cDNA, Ari Elson for the mRPTPϵ cDNA, Wouter Moolenaar for the RPTPμ cDNA, and Thea van der Wijk and Jaap van Hellemond for helpful discussions.

REFERENCES

1. Hunter, T. (1995) *Cell* **80,** 225–236
2. Neel, B. G., and Tonks, N. K. (1997) *Curr. Opin. Cell Biol.* **9,** 193–204
3. den Hertog, J. (1999) *Mech. Dev.* **85,** 3–14
4. Wang, Y., and Pallen, C. J. (1991) *EMBO J.* **10,** 3231–3237
5. Nam, H. J., Poy, F., Krueger, N. X., Saito, H., and Frederick, C. A. (1999) *Cell* **97,** 449–457
6. Lim, K. L., Ng, C. H., and Pallen, C. J. (1999) *Biochim. Biophys. Acta* **1434,** 275–283
7. Lim, K. L., Kolatkar, P. R., Ng, K. P., Ng, C. H., and Pallen, C. J. (1998) *J. Biol. Chem.* **273,** 28986–28993
8. Buist, A., Zhang, Y. L., Keng, Y. F., Wu, L., Zhang, Z. Y., and den Hertog, J. (1999) *Biochemistry* **38,** 914–922
9. Wallace, M. J., Fladd, C., Batt, J., and Rotin, D. (1998) *Mol. Cell. Biol.* **18,** 2608–2616
10. Blanchetot, C., and den Hertog, J. (2000) *J. Biol. Chem.* **275,** 12446–12452
11. Felberg, J., and Johnson, P. (1998) *J. Biol. Chem.* **273,** 17839–17845
12. Feiken, E., van Etten, I., Gebbink, M. F., Moolenaar, W. H., and Zondag, G. C. (2000) *J. Biol. Chem.* **275,** 15350–15356
13. Aricescu, A. R., Fulga, T. A., Cismasiu, V., Goody, R. S., and Szedlacsek, S. E. (2001) *Biochem. Biophys. Res. Commun.* **280,** 319–327
14. Blanchetot, C., Tertoolen, L. G., and den Hertog, J. (2002) *EMBO J.* **21,** 493–503
15. Bilwes, A. M., den Hertog, J., Hunter, T., and Noel, J. P. (1996) *Nature* **382,** 555–559
16. Desai, D. M., Sap, J., Schlessinger, J., and Weiss, A. (1993) *Cell* **73,** 541–554
17. Jiang, G., den Hertog, J., Su, J., Noel, J., Sap, J., and Hunter, T. (1999) *Nature* **401,** 606–610
18. Jiang, G., den Hertog, J., and Hunter, T. (2000) *Mol. Cell. Biol.* **20,** 5917–5929
19. Majeti, R., Bilwes, A. M., Noel, J. P., Hunter, T., and Weiss, A. (1998) *Science* **279,** 88–91
20. Alroy, I., and Yarden, Y. (1997) *FEBS Lett.* **410,** 83–86
21. Riese, D. J., and Stern, D. F. (1998) *Bioessays* **20,** 41–48
22. den Hertog, J., and Hunter, T. (1996) *EMBO J.* **15,** 3016–3027
23. Sap, J., D'Eustachio, P., Givol, D., and Schlessinger, J. (1990) *Proc. Natl. Acad. Sci. U. S. A.* **87,** 6112–6116
24. Miyawaki, A., Griesbeck, O., Heim, R., and Tsien, R. Y. (1999) *Proc. Natl. Acad. Sci. U. S. A.* **96,** 2135–2140
25. Serra-Pages, C., Saito, H., and Streuli, M. (1994) *J. Biol. Chem.* **269,** 23632–23641
26. Tertoolen, L. G., Blanchetot, C., Jiang, G., Overvoorde, J., Gadella, T. W. J., Hunter, T., and den Hertog, J. (2002) *BMC. Cell Biol.* **2,** 8
27. Weiss, A., and Schlessinger, J. (1998) *Cell* **94,** 277–280
28. Desai, C. J., Krueger, N. X., Saito, H., and Zinn, K. (1997) *Development* **124,** 1941–1952
29. Sun, Q., Schindelholz, B., Knirr, M., Schmid, A., and Zinn, K. (2001) *Mol. Cell. Neurosci.* **17,** 274–291
30. Hayami-Noumi, K., Tsuchiya, T., Moriyama, Y., and Noumi, T. (2000) *FEBS Lett.* **468,** 68–72

Intra- and Intermolecular Interactions between Intracellular Domains of Receptor Protein-tyrosine Phosphatases

Christophe Blanchetot, Leon G. Tertoolen, John Overvoorde and Jeroen den Hertog

J. Biol. Chem. 2002, 277:47263-47269.
doi: 10.1074/jbc.M205810200 originally published online October 9, 2002
